

## Self-Organization of Gold Atoms on a Polar FeO(111) Surface

Niklas Nilius,\* Emile D. L. Rienks, Hans-Peter Rust, and Hans-Joachim Freund

*Fritz-Haber Institut der MPG, Faradayweg 4-6, D14195 Berlin, Germany*

(Received 25 April 2005; published 1 August 2005)

The spatial distribution of single Au atoms on a thin FeO film has been investigated by low-temperature scanning tunneling microscopy and spectroscopy. The adatoms preferentially adsorb on distinct sites of the Moiré cell formed by the oxide layer and the Pt(111) support and arrange into a well-ordered hexagonal superlattice with 25 Å lattice constant. The self-organization is the consequence of an inhomogeneous surface potential within the FeO Moiré cell and substantial electrostatic repulsion between the adatoms.

DOI: [10.1103/PhysRevLett.95.066101](https://doi.org/10.1103/PhysRevLett.95.066101)

PACS numbers: 68.43.Hn, 68.37.Ef, 73.22.-f

The arrangement of single atoms or molecules on a solid surface is the result of a complex interplay between substrate-adsorbate and adsorbate-adsorbate interactions. On a homogeneous surface with equivalent binding sites, the interadsorbate interactions control the geometric pattern formed by the adsorbed species. While repulsive or weakly attractive forces between molecules often induce the formation of well-ordered superstructures in registry with the support, the strong adhesion between deposited metal atoms leads to the growth of compact 2D and 3D islands. Perturbations in the potential landscape for adsorption, such as point or line defects, drastically affect the spatial distribution of the adsorbates. The growth of metal particles on oxide surfaces, for example, is largely determined by heterogeneous nucleation on defect sites [1,2]. The particle distribution may also be influenced by the presence of an electronic superstructure, as observed on thin Al<sub>2</sub>O<sub>3</sub> films [3]. On various epitaxial overlayers, a dislocation network is formed via stress relief in the system, producing a regular array of nucleation sites [4]. Even charge density waves due to scattering of a surface state sufficiently perturb the adsorption potential to induce modifications in the local arrangement of CO molecules and metal atoms on noble metal (111) surfaces [5–7].

In this Letter, we report on the influence of a varying surface potential on the adsorption energy landscape as a novel parameter controlling the spatial distribution of adsorbates. Especially on polar surfaces, where a substantial surface dipole is built up by alternating layers carrying an opposite net charge, the surface free energy plays an important role in the adsorption process. Binding of atoms and molecules is assumed to efficiently relieve the surface dipole, thus stabilizing the polar surface [8–10]. Such polarity healing was experimentally identified for a number of oxide surfaces, e.g., NiO(111), MgO(111), and ZnO(0001), where it competes with extensive restructuring of the topmost layers [10–14]. Spatial variations in the surface potential, possibly induced by a modulated distance between the charged layers, would strongly affect the local arrangement of adsorbates on polar surfaces. As most

experimental results were obtained by averaging, nonlocal techniques, little is known on the interplay between a varying surface potential and a distinct distribution of adsorbed species. Apart from the academic interest, aiming for an atomistic understanding of the adsorption on polar oxide surfaces, their increased catalytic activity and superior wetting behavior with respect to nonpolar oxides warrants further investigations.

As model system for a polar oxide, we study a thin FeO(111) film where a surface dipole is built up between the Fe<sup>(+)</sup> and the O<sup>(-)</sup> layers [15–17]. The FeO surface potential is spatially modulated due to different stacking configurations of the Fe ions with respect to the Pt(111) support. The influence of such perturbations on the adsorption energy is deduced from the arrangement of single Au atoms on the FeO film, as measured with an ultrahigh vacuum STM operated at 5 K [18]. The oxide is prepared by depositing one Fe layer onto a clean Pt(111) surface at 300 K, followed by oxidation in  $1 \times 10^{-6}$  mbar O<sub>2</sub> at 950 K. The procedure results in the formation of a well-ordered bilayer of FeO(111) with O ions forming the topmost plane [15,16]. The Fe-Fe distance of 3.1 Å in the film is slightly enlarged with respect to the (111) plane in bulk FeO. The vertical separation between Fe and O layers amounts to roughly 0.65 Å, which is 50% smaller than the bulk value. This rather coplanar arrangement of positively charged Fe ions and negatively charged O ions is an effective way to reduce the surface dipole of this polar film. The lattice mismatch between FeO and Pt(111) of 3.08 Å versus 2.76 Å gives rise to a Moiré pattern with a periodicity of 25 Å [15–17]. The Moiré cell is divided into three domains, where Fe atoms alternately occupy on-top, fcc, and hcp positions on the Pt(111) [Fig. 1(a)]. The three regions are clearly distinguished by their different apparent heights in low-bias STM images [Fig. 1(b)].

A varying Fe-Pt stacking sequence is responsible for local modifications of the surface potential, as deduced from STM images taken in the near-field emission regime [19]. For a tunneling bias above the tip-sample work function, quasibound states with extremely high transmis-

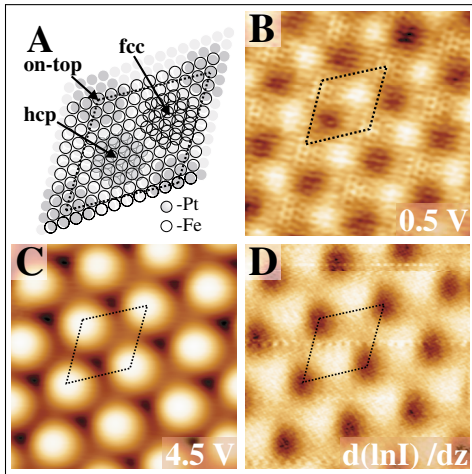


FIG. 1 (color online). (a) Structural model of the Moiré cell formed by FeO film and Pt(111). (b) STM topographic images of FeO/Pt(111) taken at 0.5 V and (c) 4.5 V sample bias. The current was set to 0.1 nA. (d) Apparent-barrier-height image of FeO/Pt(111) taken at 3.5 V sample bias. The current was set to 0.1 nA, the  $z$  modulation to 1.0 Å. All images are  $100 \times 100 \text{ Å}^2$  in size.

sion probabilities are formed in the tip-sample contact [20]. The occurrence of these field-emission resonances depends on the local surface potential, whereby the resonance condition is fulfilled first in regions with small surface barrier. Consequently, these domains are recognized by their large apparent height in STM images taken at the onset of the field-emission resonances [Fig. 1(c)]. From the contrast evolution with increasing sample bias, the bright and dark regions in Fig. 1(c) are attributed to FeO domains with small and large surface dipoles, respectively. The squared surface potential can additionally be measured by modulating the tip-sample distance and detecting the  $d(\ln I)/dz$  signal [21]. Such apparent-barrier-height maps exhibit a reversed contrast with respect to the field-emission images, demonstrating that regions where field-emission resonances occur at lower energies are, indeed, characterized by a smaller surface potential [Fig. 1(d)]. Variations of the FeO surface dipole within the Moiré cell can be connected to the modulated Fe-Pt stacking sequence using a simple hard sphere model. The largest Fe-O distance and consequently the largest dipole are expected when Fe atoms bind to hcp hollow sites and O atoms sit in on-top positions of Pt(111) (referred to as hcp domains). The minimum Fe-O distance is realized for Fe and O atoms adsorbed in on-top and fcc hollow sites of Pt(111), respectively, (referred to as on-top domains).

The effect of a varying surface potential on the adsorption behavior is deduced from the distribution of single Au atoms, deposited from a resistively heated Au wire onto the FeO film held at 10 K [Fig. 2(a)]. From the distinct apparent-height signature of hcp, fcc, and on-top domains, the Au binding sites can be identified within the Moiré cell. Four out of five adatoms in Fig. 2 are located in depressions

of the oxide film, indicating adsorption on hcp domains. The fifth atom is bound to an fcc region. The different adsorption configurations are reflected in the electronic properties of single Au atoms, as probed by differential conductance ( $dI/dV$ ) spectroscopy with the STM. The  $dI/dV$  signal is detected with a lock-in amplifier and gives a measure of the local density of states (LDOS). Conductance spectra of single adatoms adsorbed on hcp domains show a pronounced maximum at 0.5 V, which is not observed on the bare oxide film [Fig. 2(b)]. The  $dI/dV$  peak represents an unoccupied state in the LDOS of the adatom. Surprisingly, no feature is detected for Au atoms adsorbed on fcc and on-top domains, where a  $dI/dV$  signature similar to the bare FeO is obtained. Spectroscopy of occupied states below  $E_F$  reveals no  $dI/dV$  peak for single Au atoms throughout the oxide film. The spectroscopic fingerprint of adatoms located on hcp domains is exploited to discriminate the different Au binding configurations by conductance imaging. Tuning the sample bias to the  $dI/dV$  peak at 0.5 V leads to a bright appearance of adatoms on hcp regions, while atoms on other domains appear darker [Fig. 2(c)] [22]. The contrast between Au atoms in different binding positions vanishes for bias voltages above or below the resonance [Fig. 2(d)].

The specific role of hcp domains for adsorption of single Au atoms on the FeO film becomes obvious, when the coverage is increased towards one adatom per Moiré cell (0.012 ML). The majority of hcp domains is now occupied by Au atoms, which form a hexagonal superstructure with 25 Å lattice constant [Fig. 3(a)]. The power spectrum of the corresponding STM image reveals a sharp hexagonal pat-

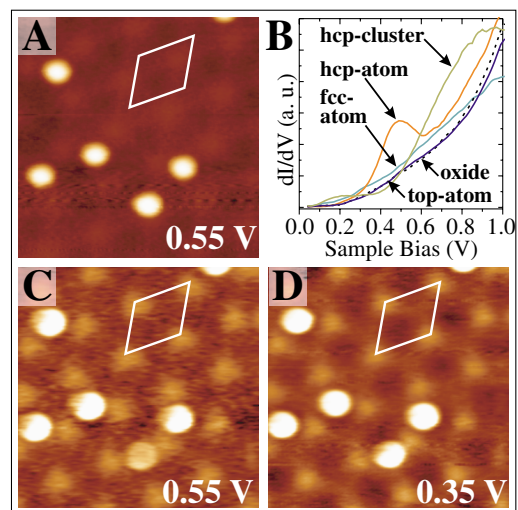


FIG. 2 (color online). (a) STM topographic image of Au adatoms on FeO/Pt(111) taken at 0.55 V and 0.1 nA. (b) Conductance spectra of bare FeO and Au adatoms bound to different domains of the Moiré cell. The tip was stabilized at 1.0 V and 0.1 nA for spectroscopy. (c) Conductance images of the same area as in (a) taken at 0.55 V and (d) 0.35 V. All images are  $130 \times 130 \text{ Å}^2$  in size.

tern, reflecting the long-range order of the atomic arrangement [Fig. 3(b)]. From  $dI/dV$  images taken at 0.55 V, the fraction of adatoms bound to hcp domains in the Moiré cell is estimated to about 60% [Fig. 3(c)]. This value is even higher when small Au clusters are included in the statistics. Gold aggregates located on hcp domains are characterized by enhanced  $dI/dV$  intensity around 0.75 V [Fig. 2(b)] and can thus be identified as protrusions in conductance images taken at elevated sample bias [Fig. 3(d)]. Counting monomers and small clusters, more than 70% of the hcp domains are occupied by Au atoms, whereas neighboring fcc and on-top regions are populated by roughly 10% each. Surprisingly, the ratio between small Au clusters and isolated adatoms remains extremely low, even when the metal coverage approaches 0.012 ML. This apparent blocking of the Au aggregation on the FeO film is in sharp contrast to the nucleation behavior observed on nonpolar oxide surfaces and indicates substantial repulsion between the adatoms [1,2,23].

The occupation characteristics of domains in the Moiré cell is further analyzed by calculating the 2D pair distribution function  $n(x, y)$  from approximately 700 adatom positions on the FeO film (Fig. 4). The highest probability to find a neighboring Au atom is along the three major FeO axes in 25 Å distance from the origin. Even 2nd and 3rd neighbor positions in the superlattice show substantial occupancy, which demonstrates the long-range order in the atomic arrangement. Maxima in the pair distribution function are split into a hexagonal substructure with 3.0 Å lattice constant, reflecting the atomic binding sites within an hcp domain. Major occupancy is observed only for 7 sites in the domain center, whereas the surrounding 12

sites are already less favored for adsorption. Based on the pair distribution function and the statistics directly derived from STM images [Fig. 3(b)], the energy landscape for Au adsorption is reconstructed from the occupation probability using a Boltzmann distribution:  $n(x, y) \propto \exp(-\Delta E/kT)$  [5,7,24]. As the adatom distribution is stable up to 50 K, the highest sample temperature accessible in the experiment, this value is used to calculate a lower bound for the energy variation  $\Delta E$ . The analysis yields an energetic preference of  $(10 \pm 2)$  meV for binding sites on hcp domains with respect to fcc and on-top regions (Fig. 4).

The observed self-organization of Au atoms can be traced back to an interplay of two characteristic properties of the polar FeO film; an inhomogeneous adsorption energy landscape with one strongly preferred binding site, and a repulsive adatom-adatom interaction suppressing the Au aggregation. The preferential adsorption on hcp domains is attributed to the large surface dipole associated with this region of the Moiré cell on the basis of field-emission and barrier-height images (Fig. 1) [19]. A large surface dipole allows effective polarization of the Au atom, increasing the interaction to the support and hence the Au binding energy. The enhanced FeO layer distance in hcp domains would also facilitate hybridization or charge transfer between adatom and support, assuming a covalent or ionic binding mechanism. The formation of a chemical bond is consistent with the appearance of the 0.5 V  $dI/dV$  peak for hcp adatoms, because pure polarization interaction would not generate a new LDOS maximum. The observed resonance is tentatively assigned to a hybridization between the Au 6s orbital and FeO electronic states,

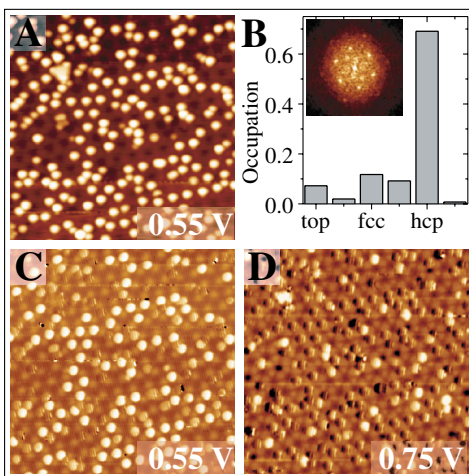


FIG. 3 (color online). (a) STM topographic image of Au adatoms on FeO/Pt(111) taken at 0.55 V and 0.1 nA. (b) Histogram of the occupation probability of different domains in the FeO Moiré cell determined from roughly 700 adatom positions. The inset shows a power spectrum of (a). (c) Conductance images of the same area as in (a) taken at 0.55 V and (d) 0.75 V. The current was set to 0.1 nA. All images are  $430 \times 430 \text{ \AA}^2$  in size.

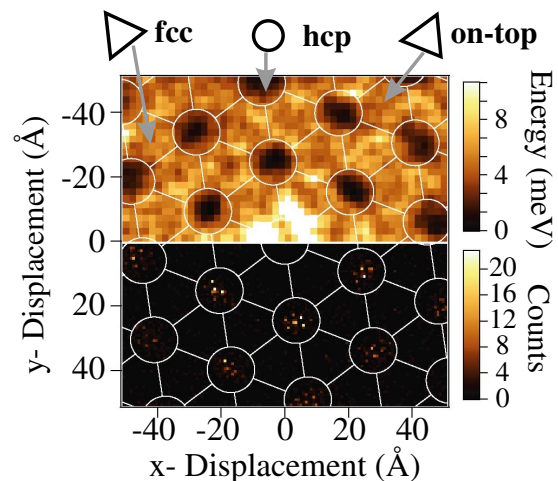


FIG. 4 (color online). Pair distribution function of Au adatoms on FeO/Pt(111) extracted from STM images at 0.01 ML Au coverage (lower part). Most events occur within hcp domains; the substructure in the distribution maxima reflects the atomic binding sites within these domains. The corresponding potential energy landscape for Au adsorption on the FeO film is calculated from the relative occupations using a Boltzmann distribution, as shown in the upper part.



giving rise to the formation of a bonding and an antibonding state. A similar mechanism was identified for single Au atoms adsorbed on NiAl(110) [25]. The antibonding state in the Au-FeO system would show up as  $dI/dV$  resonance above  $E_F$ , in accordance with the experiment. The strong spatial confinement and low tunneling probability out of filled states below  $E_F$  often hampers the detection of bonding resonances with STM [25]. Adatoms in unfavorable binding geometries would experience a less pronounced hybridization, explaining the absence of the 0.5 V peak for Au atoms on fcc and on-top domains. The preferential Au adsorption on hcp domains is additionally rationalized by the high internal surface free energy anticipated for this FeO region [Fig. 1(d)]. The Au adsorption induces a certain redistribution of charge, either by polarization or by covalent interactions, which enables partial attenuation of the FeO dipole and locally decreases the surface free energy. Such adsorption-induced stabilization mechanism has been observed for other polar oxide surfaces before [10–13].

The second requirement for a long-range ordering of the Au atoms is the adatom-adatom repulsion, which has to be active to suppress Au aggregation on the FeO film. A comparatively low aggregation tendency is not observed for metals on nonpolar surfaces, where clustering sets in at much smaller nucleation densities [1,2,23]. On the other hand, self-organization is a common behavior for alkali atoms on metal and semiconductor surfaces, where the adsorption process is accompanied by an electron transfer to the support. The positively charged alkali atoms experience substantial repulsive forces, which retard their aggregation and induce the formation of ordered superstructures [26]. The adatom interaction on the FeO film is attributed to either (i) dipole-dipole repulsion in the case that polarization interaction dominates the Au-FeO binding; or (ii) repulsion between charged Au atoms assuming partial electron transfer upon adsorption. Coulomb repulsion between equally charged atoms is generally more efficient. However, also dipole-dipole interactions would be sufficient to suppress multiple occupations of hcp domains, because of the small spatial extension of this preferential binding region. Assuming a charging of Au atoms, two competing effects will determine the direction of the charge flow. While electron transfer into the adatom satisfies the electronegative character of gold, a positive charging is more effective in healing the FeO surface dipole. Additional theoretical modeling is requested to clarify the nature of the Au-FeO bond.

In conclusion, the distinct spatial distribution of single Au atoms on FeO/Pt(111) has been traced back to a varying surface potential and a substantial adatom repulsion on this polar oxide film. The adatoms preferentially bind to sites with maximum surface dipole, where polarization as well as hybridization interactions are most effective. The reduced Au aggregation efficiency indicates Coulomb repulsion due to partial charging or polarization of the adatoms. Self-organization of single metal atoms is

expected also for other polar surfaces and opens a possibility to fabricate well-defined nanopatterns on extended oxide surfaces.

---

\*Corresponding author.

Electronic address: nilius@fhi-berlin-mpg.de

- [1] S. C. Street, C. Xu, and D. W. Goodman, *Annu. Rev. Phys. Chem.* **48**, 43 (1997).
- [2] M. Bäumer and H. J. Freund, *Prog. Surf. Sci.* **61**, 127 (1999).
- [3] C. Becker *et al.*, *New J. Phys.* **4**, 75 (2002).
- [4] H. Brune, M. Giovannini, K. Bromann, and K. Kern, *Nature (London)* **394**, 451 (1998).
- [5] M. Kulawik *et al.*, *Phys. Rev. B* (to be published).
- [6] J. Repp, F. Moresco, G. Meyer, K. H. Rieder, P. Hyldgaard, and M. Persson, *Phys. Rev. Lett.* **85**, 2981 (2000).
- [7] F. Sully, M. Pivetta, M. Ternes, F. Patthey, J. P. Pelz, and W. D. Schneider, *Phys. Rev. Lett.* **92**, 016101 (2004).
- [8] C. Noguera, *Physics and Chemistry of Oxide Surfaces* (Cambridge University Press, Cambridge, 1996); J. Goniakowski and C. Noguera, *Phys. Rev. B* **66**, 085417 (2002).
- [9] B. Meyer and D. Marx, *Phys. Rev. B* **69**, 235420 (2004).
- [10] O. Dulub, U. Diebold, and G. Kresse, *Phys. Rev. Lett.* **90**, 016102 (2003).
- [11] F. Rohr, K. Wirth, J. Libuda, D. Cappus, M. Bäumer, and H.-J. Freund, *Surf. Sci. Lett.* **315**, L977 (1994).
- [12] A. Barbier, C. Mocuta, and G. Renaud, *Phys. Rev. B* **62**, 16 056 (2000).
- [13] B. Domenichini, G. Pataut, and S. Bourgeois, *Surf. Interface Anal.* **34**, 540 (2002).
- [14] F. Finocchi, A. Barbier, J. Jupille, and C. Noguera, *Phys. Rev. Lett.* **92**, 136101 (2004).
- [15] G. H. Vurens, M. Salmeron, and G. A. Somorjai, *Surf. Sci.* **201**, 129 (1988).
- [16] Y. J. Kim *et al.*, *Phys. Rev. B* **55**, R13 448 (1997).
- [17] M. Ritter, W. Ranke, and W. Weiss, *Phys. Rev. B* **57**, 7240 (1998).
- [18] H.-P. Rust, J. Buisset, E. K. Schweizer, and L. Cramer, *Rev. Sci. Instrum.* **68**, 129 (1997).
- [19] E. Rienks, N. Nilius, H.-P. Rust, and H.-J. Freund, *Phys. Rev. B* **71**, 241404 (2005).
- [20] R. S. Becker, J. A. Golovchenko, and B. S. Swartzentruber, *Phys. Rev. Lett.* **55**, 987 (1985).
- [21] G. Binnig, H. Rohrer, C. Gerber, and E. Weibel, *Appl. Phys. Lett.* **40**, 178 (1982).
- [22] Protrusions in  $dI/dV$  images taken at 0.5 V correspond to on-top domains of the FeO Moiré cell.
- [23] G. Haas, A. Menck, H. Brune, J. V. Barth, J. A. Venables, and K. Kern, *Phys. Rev. B* **61**, 11 105 (2000).
- [24] Hot Au atoms are expected to find their equilibrium position before thermalization on the FeO film. As lateral adatom interactions play only a minor role in the Au self-organization, the 2D pair distribution function analyzes the Au-FeO interaction strength.
- [25] N. Nilius, T. M. Wallis, M. Persson, and W. Ho, *Phys. Rev. Lett.* **90**, 196103 (2003).
- [26] J. Kliewer and R. Berndt, *Surf. Sci.* **477**, 250 (2001).